The application of atomic force spectroscopy to the study of biological complexes undergoing a biorecognition process

Anna Rita Bizzarri and Salvatore Cannistraro*

Received 29th April 2009
First published as an Advance Article on the web 22nd September 2009
DOI: 10.1039/b811426a

Atomic force spectroscopy (AFS) is one of the most promising and powerful tools to get information on biorecognition processes at single molecule resolution. AFS allows to measure forces acting between biomolecules undergoing biorecognition process with a picoNewton sensitivity in near-physiological conditions and without any labelling. The capability of AFS to provide detailed information about the kinetics and thermodynamics of a single pair of interacting biomolecules, besides complementing traditional biochemical approaches, offers the possibility to elucidate non-conventional aspects of biorecognition processes, such as rare events, transient phenomena, conformational changes and molecular heterogeneity. Despite its enormous capabilities and potentialities, AFS as applied to biomolecular interactions, has provided some ambiguous and controversial results in different experimental contexts. The present *critical review* describes, after an in-depth introduction to AFS and to the most used experimental and data analysis procedures, the more recent and rewarding ideas and advancements to overcome the main critical aspects faced in the investigation of biorecognition processes. Possible developments of AFS in applicative fields are briefly addressed (150 references).

1. Introduction

Biorecognition processes involving molecules, such as proteins, DNA and lipids, play a fundamental role in life.[1] Through specific recognition mechanisms, biomolecules can build reversible, or irreversible, complexes able to perform a variety of functions, such as cell adhesion, genome replication and transcription, signalling, immune-responses, maintaining of the cell architecture, *etc*. The ability of biological molecules to undergo these highly controlled and hierarchical processes is driven by molecular-scale forces based on a combination of non-covalent interactions (*i.e*. van der Waals, hydrogen bonds, ionic and hydrophobic), which determine the strength and the characteristic time of the interactions.

Biochemistry methods have been applied to study the thermodynamics and the kinetics of complexes between biomolecular partners free in solution, or when one of them

Biophysics and Nanoscience Centre, CNISM, Facoltà di Scienze, Università della Tuscia, Largo, dell'Università-01100 Viterbo, Italy. E-mail: cannistr@unitus.it; Fax: +39 0761 357136; Tel: +39 0761 357136

Anna Rita Bizzarri

Anna Rita Bizzarri received her degree in Physics in 1987 from the University of Rome. She obtained her PhD in Biophysics in 1992 from SISSA in Trieste. After postdoctoral fellowships in Perugia and Mainz she joined the Science Faculty, Tuscia University (Italy), as a Research Assistant. In 2000 she became Associate Professor of Physics and in 2006 she became a Full Professor. Her scientific interests include spectroscopic investigations and MD simulations of electron transfer metalloproteins. More recently she has focused on single molecule level detection by surface enhanced Raman spectroscopy and scanning probe microscopies for both fundamental and applicative aims.

Salvatore Cannistraro

Salvatore Cannistraro obtained his degree in Physics in 1972 from Pisa University. He received his PhD in Biophysics at Liegi University (Belgium). In 1977 he became Reader of Biophysics at Calabria University. He moved to Perugia University in 1981 as an Associate Professor of Molecular Physics. From 1991, he has been a Professor of Physics, Biophysics and Nanoscience at Tuscia University, leading the Biophysics, Nanoscience Centre. His scientific interests lie in optical, magnetic, neutron spectroscopies and modelling of amorphous and biological systems. More recently, he is focusing his activity on the application of AFM, STM and Raman SERS to single biomolecule detection, and nanobiomedicine.

is immobilized onto a surface.[2] These techniques include rather standard approaches, with or without labelling, such as optical spectroscopies, nuclear magnetic resonance (NMR), differential scanning calorimetry and surface plasmon resonance (SPR).[3–5] However, since bulk techniques operate an ensemble averaging, they are not able to elucidate a variety of aspects inherent to individual molecules, *e.g.* rare events, transient phenomena, crowding effects, population heterogeneity, *etc.* With the advent of single molecule techniques, the study of these aspects has become accessible, offering a new and powerful tool for a deeper understanding of biological processes.[6,7] The repertoire of single molecule techniques is rapidly expanding, including optical and magnetic tweezers, biomembrane force probe, laminar flow chambers and atomic force spectroscopy (AFS).[8–12] AFS represents a particularly valuable methodology to investigate biological systems, allowing to probe intra- and intermolecular forces with high sensitivity in physiological conditions and without any labelling.

AFS can be performed using atomic force microscopy (AFM) equipment, which is a high-resolution imaging tool based on force measurements, suitable to investigate the morphological properties of biological samples without any label or sample treatments, as instead is required in confocal or electron microscopies.[13–14] AFM imaging is obtained by scanning a very sharp tip, located at the end of a cantilever spring, over the sample placed on a surface mounted on a piezoelectric scanner which is able to assure a three-dimensional positioning with subnanometer resolution.[15] The interaction force between the tip and sample is measured by the cantilever deflection which is used to create a topographical image of the sample when the tip is raster-scanned in the horizontal x–y plane.

In the AFS modality, the tip is moved only in the vertical (z) direction, perpendicular to the sample plane, downwards until it contacts the sample surface and then upwards till no tip–sample interaction is felt, by producing force–distance curves, usually in a cyclic manner.[16] The high force sensitivity (of the order of pN), together with the optimal displacement resolution (about 0.1 nm), the small probe–sample contact areas (as small as 10 nm^2) involving very few molecules, or only one, are of utmost relevance to elucidate the most subtle molecular features of biological systems. Indeed, AFS has been applied to investigate a variety of biological structures and processes, such as ligand–receptor or antibody–antigen pairwise interactions, protein unfolding, molecular stretching, conformational changes, cell deformation, membrane elasticity, adhesion between cells, *etc.* [17–23] Furthermore, AFS has a high potential for application in nanotechnology to develop innovative biosensors, especially in combination with ultra-sensitive optical spectroscopies or coupled with conductive measurements.[24–26]

To study by AFS the unbinding of interacting biomolecules forming a complex, one partner is bound to the substrate and the other to the tip; cross-linkers covalently connecting the biomolecules to the surfaces being often used.[27,28] The AFM tip is brought into contact with the surface and a complex between the partners may be formed, provided that the biomolecules have enough flexibility and re-orientational freedom to assume the correct mutual configuration. Remarkably, such a condition well mimics some real situations in which biorecognition takes place between partners, one of which is attached to a surface, such as a membrane or a cell surface.[29] When the tip is retracted from the surface, the bond between the partners is sharply broken when the applied force overcomes a threshold, usually called the ''unbinding force'' or ''rupture force''. However, since AFS measurements are performed under the application of an external mechanical force, the equilibrium energy landscape of the system is perturbed and the measured unbinding forces depend on the rate at which the force is applied, denoted the loading rate.[30] The evaluation of the equilibrium parameters from inherently non-equilibrium pulling experiments, can be done within appropriate theoretical approaches.[31] In the framework of the Bell–Evans phenomenological model, which assumes a decrease of the activation barrier proportional to the applied force, the dissociation rate, k_{off}, of a complex and the energy barriers can be extracted from an analysis of the unbinding force as a function of the loading rate.[32]

Although AFS has demonstrated enormous capabilities to provide detailed information on biological complexes, at single molecule level, the occurrence of some ambiguous and controversial results has been registered in different experimental and modelling contexts. Therefore, great care should be exercised in both experimental and analysis procedures in order to eliminate possible drawbacks and artifacts which might spoil the success of AFS. In the following, we will address some issues whose control is crucial to obtain the most reliable results from AFS, applied to the study of biorecognition process.

(i) Single molecule biorecognition studies require that only an individual pair of interacting biomolecules is effectively involved in the unbinding process. The occurrence of sequences of multiple bond ruptures, or detection of large unbinding forces, could be indicative, instead, that a number of molecules participate to the unbinding process. To provide a reliable description of the unbinding processes, a control of the immobilization procedures of the biomolecular partners to the tip and the substrate, respectively, is strongly required to limit, at the best, multiple events. Furthermore, data analysis procedures, able to well-discriminate single molecule events from multiple ones, are highly desirable.

(ii) The AFS data are often affected by the presence of unbinding events related to nonspecific interactions between the probe and the substrate. These events may arise from an improper spatial orientation of the partners, inappropriate contacts, or nonspecific adhesions between the functionalized tip and the substrate, even without the involvement of biomolecules. Accordingly, it is of utmost importance to establish criteria which allow to reliably discriminate between specific and nonspecific interactions by recognising false positive events.

(iii) Although the Bell–Evans phenomenological model has been successfully applied to describe the trend of the unbinding force as a function of the loading rate for several biomolecular complexes,[33–38] the observation of some contradictory or scattered results has stimulated some corrections, or further developments, of this model.[39,40] Along this direction, an intense activity has been devoted to better understand the

mechanisms involved in the unbinding processes under the application of an external force (see *e.g.* refs. 41 and 42). Additionally, alternative theoretical approaches to derive the equilibrium free energy from mechanical work performed in non-equilibrium measurements, has recently opened a new perspective in the study of biological systems.[43]

On such a basis, we wish to critically revisit the applications of AFS to investigate biological complexes, at the single molecule level, by especially focusing the attention on recent ideas and advancements on both the experimental and data analysis procedures, which offer solutions to overcome the above mentioned critical aspects. In particular, the strategies developed to immobilize the interacting biomolecules, in order to favour a correct interaction between them, to reduce multiple events, and to discriminate between specific and nonspecific unbinding events will be reviewed. Additionally, the current methodologies to analyze the force curves, and the main theoretical models to extract kinetic and thermodynamical quantities from AFS data will be outlined. Finally, the potentialities of AFS in applicative fields, especially for ultra-sensitive detection, even in combination with other single molecule techniques, will be briefly addressed.

The review is organized as follows. In section 2, the kinetics of biorecognition is briefly discussed also in connection with the capabilities of AFS and of other, related single molecule techniques, to provide information on the mechanisms underlying the formation of biological complexes. In section 3, the AFS technique is briefly described with a particular focus on those experimental aspects relevant to study the unbinding processes of interacting biomolecules. The methodologies and the emerging solutions to immobilize the two biomolecular partners to the AFM tip and the substrate, are reviewed in section 4. Section 5 provides an overview of the main features characterizing the force–distance curves of the unbinding processes and of the corresponding data analysis procedures. The theoretical models currently used to analyze the unbinding forces in order to extract kinetics and thermodynamics information, are presented in section 6. Finally, a brief summary together with additional, upcoming capabilities and potentialities of AFS to investigate single biomolecular complexes, are considered in section 7.

2. Biorecognition processes

Biorecognition plays a central role in life. A large part of functions in a cell resides in the recognition between biomolecules and the subsequent formation of specific molecular associations held together by a collection of non-covalent bonds. Upon undergoing a biorecognition process, biomolecules give rise to an extremely wide variety of associations with very different properties: from antigen–antibody complexes characterized by a tight binding, long life-times and high specificity, to short-lived transient complexes formed by molecules that recognize multiple partners, often with a charge transfer capability.[44–46] Biorecognition has been widely studied from both experimental and theoretical points of view,[47] however many aspects of how it works are still debated. For example, the capability to predict the structure of a biomolecular complex, if the single components are known, remains a challenging task of theoretical biology.[48] The molecular mechanisms underlying biorecognition processes can be described within different frameworks. The "Lock and Key" theory takes into account an almost perfect fit between the partners whose shapes are assumed to be rather rigid.[49] At variance, the "Induced-fit" theory assumes that one partner, *e.g.* the ligand, plays a role in determining the final shape of the other one, *e.g.* receptor, which is partially flexible.[50] Alternatively, a mechanism has been recently proposed for which proteins adapt their structure to different binding partners through a conformational selection arising from structural heterogeneity thermally accessible in solution.[51] A quantitative description of a biorecognition process requires a kinetic treatment. When two molecular species A and B with mutual affinity are mixed in a solution, their association, AB, satisfies the following time-dependent equation:

$$\mathrm{d[AB]}/\mathrm{d}t = k_{\mathrm{on}}[\mathrm{A}][\mathrm{B}] - k_{\mathrm{off}}[\mathrm{AB}] \quad (1)$$

where the square brackets stand for the concentration of the molecular species, k_{on} and k_{off} are the association and dissociation rates of the complex, respectively, which describe the kinetics of the interaction. The k_{on} parameter is mainly related to the diffusive properties of the biomolecules, with some dependence on the distance and orientation between the partners.[52] By contrast, k_{off}, which is related to the characteristics lifetime τ_{o} of the complex ($\tau_{\mathrm{o}} = {k_{\mathrm{off}}}^{-1}$), provides more information on the specificity of the reaction.

In the framework of the Kramer's theory, for a reaction in which the bound and the unbound states are separated by a single energy barrier proceeding through a specific path along the reaction coordinate, k_{off} is given by an Arrhenius-like expression:[53]

$$k_{\mathrm{off}} = w\exp(-\Delta G^*/k_{\mathrm{B}}T) \quad (2)$$

where ΔG^* is the activation free energy of the reaction (*i.e.* the difference in free energy between the initial state and the transition state of the highest energy to which the system must be raised before dissociation can occur (see Fig. 1)), k_{B} is the Boltzmann constant, T is the absolute temperature and w is the pre-exponential factor which is usually taken as temperature independent. The reaction between A and B will tend to an equilibrium state ($\mathrm{d[AB]}/\mathrm{d}t = 0$), by following the mass action law:

$$\frac{[\mathrm{AB}]}{[\mathrm{A}][\mathrm{B}]} = \frac{k_{\mathrm{on}}}{k_{\mathrm{off}}} = K_{\mathrm{a}} = \frac{1}{K_{\mathrm{d}}} \quad (3)$$

where K_{a} and K_{d} are the association and dissociation constants, respectively. A high value for K_{a} is indicative of high affinity between the two molecular species A and B.

From the relationship $K_{\mathrm{a}} = k_{\mathrm{on}}/k_{\mathrm{off}}$, it comes out that the same K_{a} value could arise from different values of k_{on} and k_{off}. Accordingly, two complexes could be characterized by similar affinity, but different timescales. While such an aspect is not relevant at equilibrium, it could play a crucial role if the temporal course of a reaction has some interplay with other processes, as happens in biological systems. In other words, biomolecular interactions could be not necessarily optimized to achieve the highest affinity, but they could have been

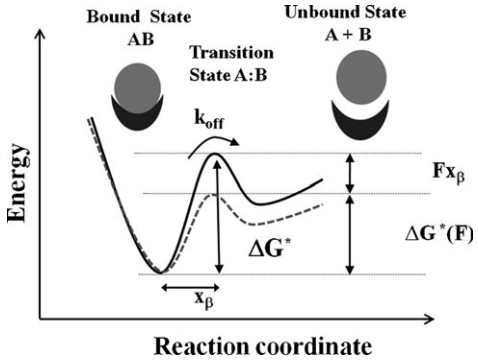

Fig. 1 A schematic diagram of the energy profile for a dissociation process of a biomolecular complex without an external force (continuous line) and under the application of an external force F (dashed line). ΔG^* and $\Delta G^*(F)$ are the corresponding activation free energies.

selected to reach the best result in a short time.[52] For example, maturation processes of antibodies select those biomolecules characterized by a high association rate, *i.e.* high k_{on}, able to target antigens rapidly, instead of promoting complexes with high affinity.[54] On the other hand, the different responses of T lymphocytes to bind protein ligands having almost the same affinity, can be traced back to a different dissociation rate.[55] A detailed investigation of k_{on} and k_{off} is, therefore, of utmost relevance for a full understanding of the mechanisms underlying the biorecognition process between biomolecular partners.

Classical biochemistry methods, usually applied to investigate the interaction of biomolecules in solution, include a wide range of techniques. In particular, the absorption and emission of optical signals, even implemented in stopped-flow setups, can be monitored to extract thermodynamics and kinetic constants.[2] However, these types of measurements can provide only a description in bulk. This means that some aspects, such as transient phenomena, rare events, conformational changes, population heterogeneity, crowding effects, influence of compression from adjacent cells, *etc.*, cannot be elucidated since they are hidden in the ensemble average. At the same time, biomolecular interactions probed in solution might be not representative of processes occurring in two dimensions, *i.e.* when one, or both the biomolecules are anchored or embedded on a cell surface. In these cases, the biomolecules may undergo a restricted motion which could affect their biorecognition capability and kinetic response.[56,57] Even if now there are available techniques, such as SPR, which allow to investigate kinetic properties of molecular complexes, when one of the partners is immobilized onto a surface, a full characterization of these processes may not be achieved because they interrogate samples containing a large number of biomolecules.[58] In this respect, the capability of innovative techniques to investigate biological systems by scaling down to single molecule level could constitute a rewarding tool complementing biochemical approaches. Among single molecule techniques, AFS has the advantage to sense interaction forces with an extremely high sensitivity (pN) and to allow the evaluation of the dissociation rate k_{off}, in near-physiological conditions and without any labelling, even for an individual, immobilized couple of interacting biomolecules. In addition, AFS permits to estimate the number and the height of the energy barriers involved in the unbinding processes.[32,43]

The study of biorecognition processes by AFS can take advantage from a comparison with the results from other, related single molecule techniques, such as flow chambers, optical trappings and biomembrane force probe.[6,52,59] In particular, biomembrane force probe, which exploits the deformation of a microvesicle under tension as a force sensor, used in combination to AFS, has contributed to resolve the ambiguities which have arisen in the study of the streptavidin–biotin complex[60] (see also section 5).

3. Overview of the AFS technique

AFS measurements are performed by an AFM equipment consisting of a cantilever (rectangular or V-shaped), usually made of silicon or silicon nitride, with a sharp tip held above a piezoelectric scanning stage on which the sample is mounted, as schematically shown in Fig. 2;[61] the tip having a radius of curvature on the order of nanometers. In an alternative setup, the cantilever, rather than the sample, can be moved by the piezoelectric translator.[15] The AFM apparatus can operate in vacuum, in air and in liquid, including physiological buffers. The scanner can be moved in three dimensions by a subnanometer amount when a voltage is applied. The resolution in the vertical (z) direction is tenths of angstroms, and is limited by thermal noise, while the resolution in the x–y plane is a few nanometers, being generally limited by the tip curvature radius.[15] The tip–sample interactions, arising from a variety of forces (electrostatic, van der Waals, frictional, capillary, chemical, *etc.*), yield a cantilever deflection, d, which is detected by using a laser beam bouncing off the back of the cantilever onto a position-sensitive photodetector (providing current or voltage readings) (see Fig. 2).[62,63]

To form an image by AFM, two main operating modes can be used: static or contact mode and dynamic mode. In contact mode, the tip is brought close to the sample and then it is raster-scanned over the surface by applying a constant force through a feedback mechanism. By detecting the cantilever deflection, due to probe–sample interactions, a mapping of the surface characteristics at sub-nanometer resolution can be obtained.

In the dynamic mode, the cantilever interacts intermittently with the sample. In particular, in tapping mode, images can be acquired by putting the cantilever in oscillation with a

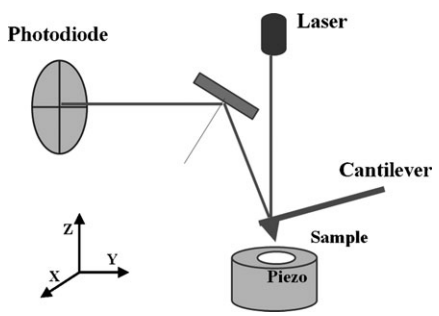

Fig. 2 Scheme of the main components of AFM apparatus.

frequency close to its resonance frequency, at an amplitude typically between 100 to 200 nm; the surface being raster-scanning by maintaining the amplitude constant through a feedback.[64] Since the tip touches the sample only at the end of its downward movement, sample damage by scanning the probe is greatly reduced. For this reason, the tapping mode is commonly preferred for studying biological systems.[65] A detailed description of AFM principles and applications to biological systems can be found in refs. 14, 15 and 66–68.

An AFM apparatus can be used as a force measuring device in the modality usually called AFS. The deflection of the cantilever provides a readout of the force exerted on the sample, while the displacement between the surface and the tip is simultaneously controlled. More specifically, at a fixed location of the x–y plane, the piezo-scanner is moved, at a constant speed with respect to the substrate in the vertical direction (z) toward the tip and backwards. The deflection of the cantilever, recorded as a function of the vertical displacement z, in a cyclic way, is usually called a force curve. When the tip and the sample are well separated, no interaction is sensed between them; while at shorter separation, the tip–sample interaction results into a cantilever deflection (a detailed description of the force curves will be given in section 5). Within an approximate harmonic potential, the deflection of the cantilever, d, can be then converted into a force value through the Hooke's law, $F = kd$. Accordingly, an experiment performed at a constant speed, v, is characterized by a constant loading rate, $R = \mathrm{d}F/\mathrm{d}t = kv$. The effective value of the cantilever spring constant k may be generally different from the nominal one provided by manufacturers. Several experimental procedures to evaluate the spring constant k have been developed.[15,69] A common method consists of attaching a known mass at the end of the cantilever and to measure the resulting change in its resonance frequency.[70] Alternatively, the stiffness of the cantilever can be obtained through comparison with a reference cantilever. One of the most used methods, implemented in many commercial AFM equipments, is based on cantilever thermal noise analysis.[71]

The cantilever of unknown spring constant k, is modelled as a harmonic oscillator and undergoes random fluctuations due to thermal vibrations. k can be calculated by measuring the mean square deflection $\langle d^2 \rangle$, through the equipartition theorem, $k = k_{\mathrm{B}}T/\langle d^2 \rangle$, where k_{B} is Boltzmann constant and T the absolute temperature. For AFS measurements, cantilevers with small spring constants (usually in the range 10^1–10^2 pN nm^{-1}) and short lengths (< 50 μm) are preferred since they are characterized by lower force noise.[72] Noticeably, the cantilever spring constant k, can be modified due to the functionalization with one of the biological partners.

The accuracy in the measurements of the displacement along the z direction can be affected by the nonlinear trend with the voltage, connected with drift, hysteresis and creep, of the piezo-electric actuators;[73] this may compromise a precise positioning of the sample. The introduction of closed-loop feedback scanners has practically eliminated these problems by allowing to accurately determine the position of the tip with respect to the sample.

4. Biomolecule immobilization strategies for unbinding experiments

To study the interaction between biomolecules undergoing a biorecognition process, one partner is bound to the apex of AFM tip, while the other one is immobilized on the substrate (see Fig. 3).

These immobilization procedures should satisfy some general requirements:[6,16] (i) The anchoring of the biomolecules to the inorganic surfaces (tip and substrate) must be stable and stronger than the intermolecular forces holding the complex to be studied. To such an aim, covalent bonding is usually preferred. (ii) The native structure and functionality of the biomolecules are to be preserved, at the best, upon their immobilization onto the solid surfaces. (iii) Despite the engagement of part of the biomolecule in the covalent attachment, the interacting regions of both the partners should remain available for their recognition.

At the same time, the biomolecules should retain a sufficient mobility and re-orientational freedom to favour a recognition process. (iv) Nonspecific interactions between the functionalized tip and the substrate should be avoided, or minimized, in order to limit the presence of artifacts. (v) Finally, the immobilization strategies should ensure that a single couple of interacting biomolecules is analyzed at each time. In this connection, a special attention should be devoted to check the environmental conditions (such as the pH, ionic strength, density and orientation of the biomolecules on the surfaces), as well as to assure a high purity of biomolecules.

In the last few years, the above-mentioned requirements have resulted in considerable efforts to develop strategies able to properly attach the biomolecules to the surfaces *via* covalent or noncovalent bonding with the support of surface chemistry techniques. The most commonly used substrates are constituted by silicon, glass, mica and gold. In the first pioneering AFS experiments, an immobilization of the biomolecules directly on the surfaces (tips or substrates) has been achieved (see Fig. 4).[16] For example, proteins that carry a net positive charge at the working pH conditions, can be immobilized electrostatically on freshly cleaved mica which is negatively charged.[37,74–76] On the other hand, biomolecules can be

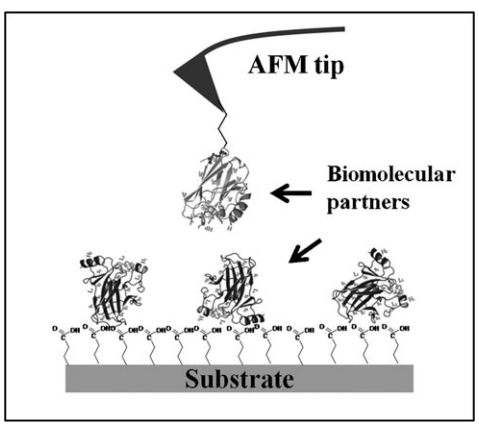

Fig. 3 Schematic representation of the AFS setup for an unbinding experiment of a biomolecular complex. Both the partners are immobilized to the surfaces (tip or substrate) by flexible spacers.

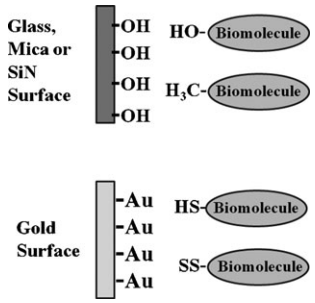

Fig. 4 Representation of the main strategies to directly anchor biomolecules to inorganic surfaces (tip and substrate).

directly immobilized on the tip, usually made of silicon or silicon nitride, or even on glass substrate, *via* a reaction of specific groups of biomolecules (mainly, oxydryl or methoxy) with the oxydryls of the surfaces, available directly or after chemical or physical treatment.[12,29,77]

Furthermore, biomolecules can be anchored on gold substrates through their exposed, native or engineered, thiol groups, thanks to the gold capability to form covalent bonds with sulphur atoms.[78–80] We note on passing that the use of conductive substrates in AFS experiments, allowing to achieve a good electric conduction through the molecule toward the substrate, makes feasible to combine AFS with conductive measurements, *e.g.* by scanning tunnelling microscopy (STM) or conductive-AFM, in the perspective of multisensing detection.[26]

Thiol groups can be also exploited to anchor biomolecules on tips, upon coating their apex with a thin layer of gold (50–100 nm).[81]

Today, the use of short and rigid, or longer and flexible (or even a combination of both) cross-linkers is widely preferred to connect inorganic surfaces with biomolecules. In general, the introduction of linkers has several advantages. (i) Linkers, placing biomolecules at a certain distance from the solid surface, can prevent distortions and denaturation due to a direct biomolecule–surface interaction.[82,83] (ii) In the presence of linkers, specific unbinding events take place far away from the sample surface, while the nonspecific ones remain near the tip–surface interface.[84,85] (iii) The presence of flexible linkers endows the biomolecules with both an increased mobility and a re-orientational freedom that may favour an optimized recognition between the partners. (iv) A flexible linker undergoes, during the tip-retraction, a stretching process whose peculiar features can help to discriminate between specific and nonspecific unbinding events (see also section 5).

Linkers are heterobifunctional molecules, often polymers, which carry two different functional ends, one to link the inorganic surface and the other to target specific functional groups of the biomolecule, or of another linker.[16,29] Some preparation protocols involve a preliminary functionalization of the surfaces with self-assembled short spacers with one end suitable for reaction with the surfaces, and the other for reacting with other molecules (linkers or biomolecules). For example, gold, or gold-coated surfaces (substrates or tips) can be functionalized with alkanethiols, such as cysteamine, bearing, at one end, a thiol group having a high affinity for gold and the other with a group able to target the biomolecules.[26,86] Glass substrates, silicon or silicon nitride tips, after a chemical or physical treatment to expose oxydryl groups, can be functionalized with silanes, or alcohol-based spacers, such as ethanolamine.[87,88] The most used reacting groups within the available protocols for tip and substrate functionalization are summarized in Scheme 1.

One of the mostly used flexible linker in AFS is the heterobifunctional poly(ethylene glycol) (PEG).[28,84,89] PEG is a versatile polymer, with well-characterized stretching properties, which can be synthesized at different lengths and bearing different functionalized ends.

Other types of molecules, such as DNA, antibodies, amino-acids, oligomers (*e.g.* Titin domains), have been employed to provide a bridge between inorganic surfaces and biomolecules.[90–94] Again, the stretching features of these molecules provide some help to discriminate between specific and nonspecific unbinding events.[28,95] Alternative protocols exploit nitrilotriacetate (NTA)-terminated linkers, able to target histidine, together with recombinant histidine-tagged proteins.[96,97] In this way, all the biomolecules are uniformly oriented and possess a good flexibility which favours the interaction between the partners.[96] However, the low binding strength (150–200 pN) limits its applicability in the study of

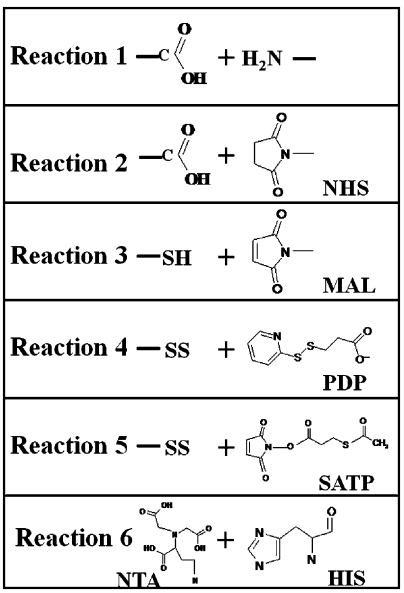

Scheme 1 *Reaction 1*: A carboxyl function can be reacted with amino groups belonging to proteins (or to linkers), using 1-ethyl-3-(3-dimethylaminopropyl) carbodiimide (EDC) and *N*-hydroxysuccinimide (NHS) in aqueous solution.[81] *Reaction 2*: Molecules ending with the NHS function can be reacted with amino groups in presence of EDC.[81] *Reaction 3*: Maleimide (MAL)-terminated polymers can form a stable carbon–sulfur bond with a thiol group, in the presence of a solution of *N*-succinimidyl 3-maleimidopropionate (SMP).[26] *Reaction 4*: Polymers ending with 2-pyridyldithiopropionyl (PDP) can be reacted with a sulfur group.[86] *Reaction 5*: Polymers terminated with *N*-succinimidyl-*S*-acetylthiopropionate (SATP), can be reacted with disulfide moieties of proteins after deprotection of SATP with a solution of hydroxylamine, ethylenediaminetetraacetic acid (EDTA), and dithiothreitol (DTT).[83] *Reaction 6*: Nitrilotriacetate (NTA)-terminated spacers can react with histidine residues.[96]

some biological complexes.[16] Finally, we mention an interesting strategy exploiting the properties of functionalized carbon nanotubes, for specific attachment of single molecules.[98]

As above stated, an ideal AFS unbinding experiment should involve possibly a single couple of interacting biomolecules. In this respect, substrate and tip, when functionalized at low coverage, certainly favour the occurrence of a single rupture events. However, many AFS experiments have been performed with a full coverage of biomolecules on the substrate, and a low density of the partner on the tip. These conditions, besides favouring multiple events, can also give rise to some steric hindrance, with some hampering of the binding process. Nowadays a low biomolecular coverage also on the substrate is preferred.[99] To achieve a controlled density of partners on the surfaces, functionalization strategies using a mixing of linkers with different capability to target biomolecules, have been implemented. For example, linkers bearing at one end a protein-resistant group (*e.g.* oligo-(ethylene glycol) (OEG)) can be mixed with linkers able to target specific groups of the protein, such as NHS (see also Scheme 1).[100,101]

The functionalization of the substrate should be preliminarily checked to verify that biomolecules have been effectively immobilized on it. To this purpose, several approaches have been followed, including enzyme immunological assay to verify the protein activity, X-ray photoelectron spectroscopy to analyze the surface chemical composition and AFM imaging to analyze the morphological properties of the substrate.[99]

To visualize isolated biomolecules by AFM imaging, the use of substrates with a low roughness, such as bare mica or annealed gold substrates, are preferred. The height of the AFM imaged spot can be then compared with the expected dimensions of the biomolecules in order to obtain some information on possible structural deformation.[102] On the other hand, for substrates with high molecular coverage, the thickness of the molecular film can be evaluated by performing scratching by AFM in contact mode and compared with that expected from a single biomolecular layer.[97,103]

As already mentioned, a correctly designed immobilization should take into account that the biomolecular regions involved in the formation of the complex have to remain available to undergo a biorecognition process. However, when these interacting regions are not known, for example because the crystallographic structure of the complex is lacking, computational docking procedures can be used to predict the most probable configuration of the complex. Conventional docking, starting from the three-dimensional structures of the individual partners, probes the full surfaces, looking for all the possible binding modes.[104] These obtained complex configurations are ranked according to a scoring function, which takes into account one or more criteria (geometric, electrostatic, energy interactions *etc.*).[44,48] The complexes with the highest scores are further refined by applying further criteria on the basis of experimental indication (*e.g.* mutagenesis) in order to extract the best complex. The prediction of the final structure of the complex can be then exploited to develop immobilization procedures able to place the biomolecules with a well-defined orientation on the surfaces.[46,105,106]

5. Unbinding experiments on biomolecular complexes

5.1 Force curve analysis

To measure the unbinding force in a pair of interacting biomolecules by AFS, the tip functionalized with one of the biomolecules is approached, at a constant speed, towards the partner-coated substrate; then, the tip is retracted to reach the initial position. During an AFS experiment, a large number of force curves (hundreds or thousands) are acquired, often in a cyclic way, at the same, or at a different (x, y) position.

A representative force–distance cycle is shown in Fig. 5. At the beginning, the functionalized tip is far away from the coated substrate, so there is no interaction, and no cantilever deflection is recorded (point A). As the tip is approached towards the substrate and the two biomolecules become closer, the interaction forces begin to act causing a deflection of the cantilever toward the sample for attractive forces (point B) (or away from the sample in the case of repulsive forces). During such a step, the tip and the substrate jump-to-contact. If the two partners have enough flexibility and re-orientational freedom to assume a correct reciprocal orientation, they undergo a biorecognition process forming a specific complex.

A further pushing the tip on the substrate yields a higher cantilever deflection due to mutual electronic repulsions between overlapping molecular orbitals. Such a region, which is typically linear (from point B to C) provides information to convert the photodiode current or voltage into the cantilever deflection through the sensitivity of the detector.[107] The approaching phase is stopped (point C) upon reaching a preset maximum value of contact force (F_c) between the tip and the sample; such a value being usually kept below 1 nN to avoid damage of the sample. Then, the direction of motion is reversed and the tip is retracted from the sample with a speed that can be set at different value with respect to that applied in the approaching phase. During the retraction, adhesion forces, and/or bonds, formed in the contact phase, cause the tip to adhere to the sample up to some distance beyond the initial contact point, and the curve shows a hysteresis (from point

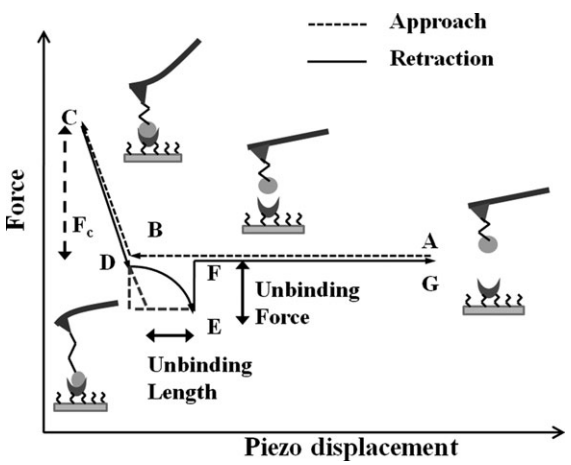

Fig. 5 Schematic diagram of a typical AFS force curve representative of a specific unbinding event for a single biomolecular complex.

D to E). As the retraction process continues, the spring force overcomes the interaction forces and the cantilever pulls off sharply, going to a non-contact position (jump-off-contact) (point F). Such a jump provides a measure of the unbinding force (also called the rupture force) between the partner biomolecules. Values of unbinding forces below 15 pN are usually assumed to be not significant, due to the signal-to-noise ratio of commercial AFM apparata.[16]

The approach of a functionalized tip toward a coated substrate does not necessarily result into the formation of a specific complex. Actually, an improper spatial contact between the biomolecules, or even an interaction between the tip and the substrate without the involvement of one, or both, the biological partners, may give rise to nonspecific interactions. In these cases, of course, the jump-off-contact does not provide information about the specific force between the partners. Therefore, large efforts have been devoted to develop criteria helping to reliably single out force curves corresponding to specific unbinding events. Such a task is somewhat difficult, since the real curves exhibit a sort of "zoology" of different shapes and trends.[34,103] A few representative examples of curves are shown in Fig. 6.

Curve 1 does not show any detectable unbinding event, since the retraction follows faithfully the approach. Curve 2 shows the occurrence of a jump-off-contact event, however, the curve retains the same slope during the retraction in the contact region. This can be attributed to a nonspecific adhesion between the tip and the substrate, likely without the involvement of the biomolecules and the corresponding force

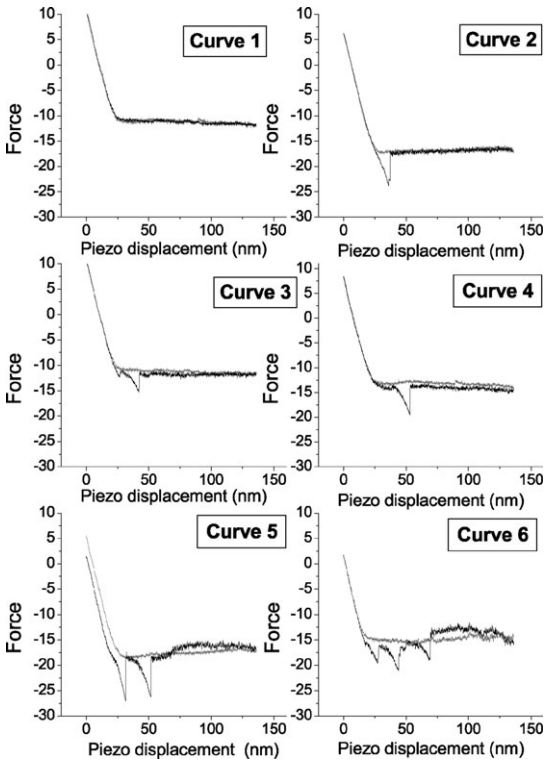

Fig. 6 Real AFS force curves for a biomolecular complex. Curve 1: no event, curve 2: nonspecific event since the linear slope of the retrace extends beyond the contact line; curves 3 and 4: specific unbinding events; curves 5 and 6: multiple events. For more details see the text.

curve is discarded.[85] Curves 3 and 4, instead, show a trend qualitatively reminiscent of that shown in Fig. 5, in which the slope of the curves changes during the retraction process. This is indicative that, at the beginning of the retraction process, the cantilever is relaxed, while during further retraction, the system becomes stretched.[28,85] Such a behavior is commonly attributed to specific events, especially when flexible linkers are used to immobilize the biomolecules to the tip or to the substrate.[37,108] In this case, the unbinding length, evaluated from the nonlinear portion of the retraction curve (see Fig. 5) is expected to almost match that of the linker under stretching.[37] The stretching curve of the flexible linkers, suitably modeled in terms of a worm-like chain or freely joined chain, should be superimposed to the experimental extension trace of the force curve preceding the jump-off-contact.[97,109,110] A good agreement between the fitted and the experimental extension traces is assumed to be a fingerprint for specific events.[93,111] Notably, in the presence of long elastic linkers, specific unbinding events occur far away from the sample surface, while the non-specific ones remain near the tip–support interface.[34,38,85,100]

Curves 5 and 6 show examples in which several jumps are detected along the retraction. These jumps may reflect a variety of phenomena: multivalent specific interactions, partial stretching of the molecules, nonspecific interactions *etc*.[34] When multiple jumps are observed, it is common to attribute a force curve to a specific unbinding event if the last jump is starting and ending at zero deflection; the last jump being taken as representative of the unbinding process.[37] On such a basis, curve 5 is accepted, while curve 6 is discarded.

5.2 Statistical analysis of unbinding forces

Generally, the large variability observed in the force curves can be traced back to the stochastic nature of the unbinding process in the single molecule limit.[87] To extract reliable quantitative information, a statistical analysis of a large number of force curves should be performed. In this respect, a crucial aspect is represented by the selection of force curves related to specific events, then discarding curves which can be attributed to nonspecific ones; ambiguous curves being also discarded to avoid the introduction of potentially 'false events'. Such a selection should be carefully done by applying appropriate and reliable criteria, such as those mentioned in section 5.1.

Upon selecting the curves related to specific events, the unbinding frequency, given by the ratio between successful events (*i.e.* events corresponding to specific unbinding processes) over the total recorded events, can be evaluated. Unbinding frequencies ranging from 15% to even 85%, have been registered for different biomolecular complexes.[38,95,96,107,112–115] Noticeably, the unbinding frequency may depend on the immobilization chosen for the interacting biomolecules.[80] Control experiments in which the biorecognition process is inhibited, are used to confirm the specificity of the detected unbinding events on statistical grounds.[12,95,107] This is achieved by saturating the tip or the substrate with the complementary blocking agent (*i.e.* the partner). A significant decrease (about 50%, or more) of

the unbinding probability is expected to be observed for a specific unbinding experiment. The persistence of a residual activity after blocking has been detected for several systems, even in very effective blocking conditions;[28,38,95,115] such a residual activity can be likely ascribed to the forced interaction between the two molecules in the experimental setup.

Other kinds of experiments have been suggested to further support the specificity of the unbinding events. For example, if one of the partners is removed from the experimental setup or even substituted with a noninteracting one, then the disappearance of specific events can be checked.[116] Interestingly, the AFS technique has been also used to investigate the competition of among two, or even more ligands for the same binding site.[117,118]

The unbinding forces extracted from a collection of curves assigned to specific events, are usually plotted as histograms; the binding of the force values being normally kept higher than 5 pN. The resulting distributions are generally asymmetric and more or less spread, with single or multiple peaks (see Fig. 7 and the related inset).[41,89]

This variability of the unbinding forces could be generally ascribed to several factors, such as heterogeneity in the formation of the complex, slight differences in the relative arrangements of the partners, existence of different binding sites, occurrence of multiple unbinding processes, *etc*.[34,119] Notably, the unbinding force distributions, before and after blocking, often exhibit almost the same shape (see Fig. 7). In this case, the survived unbinding events can be assumed to be of the same nature of the events recorded before blocking, in agreement with the hypothesis that the residual specific activity after blocking is due to the forced interaction between the partners.[38,95,103]

The presence of clearly distinct peaks in the histograms has been ascribed to the occurrence of multiple unbinding events, *i.e*. a synchronous unbinding of more than one pair connected in parallel.[12] In particular, when the peaks in the distribution are equally spaced (see inset of Fig. 7), the distance between two subsequent peaks has been assumed as the quantum for the unbinding force.[12,36,103] However, analysis of multiple peaks requires a special care since multiple unbinding events could arise from different configurations in the experimental setup. Biomolecules could be connected serially, in parallel or in a zipper sequence.[101,120,121] Besides the connection, the effective number of interacting molecules should be known in order to reliably analyze the data. For example, when n biomolecular pairs are pulled at the same time, the effectively applied loading rate could be shared among them; *i.e*. the real loading rate could be $1/n$ the global value.[34,120] To gain some information about the spatial organization of the biomolecules, it has been suggested to repeat the experiments by varying some parameters, such as the density of the biomolecules or the linker length. However, the main difficulty in interpreting multiple bond measurements resides in the lack of a reliable way to determine the number of the involved biomolecule pairs.[101] It is therefore extremely important to restrict the possibility that multiple events may take place, adopting immobilization strategies which allow to approach the single molecule limit.

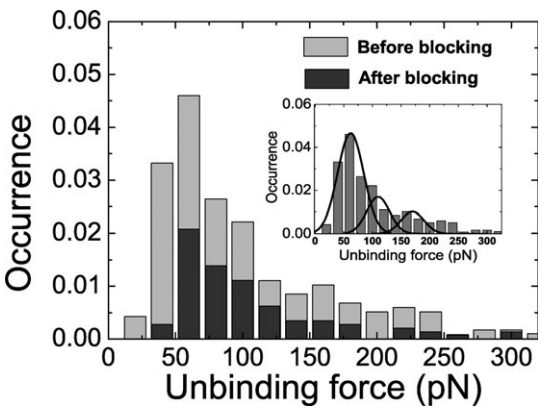

Fig. 7 Example of unbinding force distributions of events recorded, at loading rate of about 3 nN s^{-1}, before and after blocking (data from ref. 38). Inset: example of multiple unbinding force distributions of unbinding events recorded (data from ref. 103). The histograms were fitted to Gaussian functions to identify the most probable unbinding force values.

From an histogram collecting several specific unbinding force values, at a given loading rate, the most probable unbinding force can be extracted.[122] For a single mode distribution, such a quantity is often evaluated from the maximum of the distribution or, if appropriate, by a fit with a Gaussian function. When multiple peaks are observed, the most probable unbinding force is usually evaluated from the first peak. However, more accurate and refined procedures to analyze the force distributions in the presence of multiple unbinding events have been developed by simultaneously taking into account both the unbinding forces and lengths, even in connection with the elastic characteristics of the used spacers.[101,123]

Since the analysis of the force curves requires to manage a very large amount of data, it can be significantly simplified and shortened if routine analysis procedures are implemented. To such a purpose, the integration of well-defined criteria to calibrate force distance data, peak detection, histogram construction *etc*. should be implemented in an automatic procedure. Along this direction, two attempts have been recently developed to analyze AFS force curve data.[116,124]

Generally, the unbinding force depends on the number, the strength, and the directionality of the noncovalent bonds involved in the interaction. Furthermore, it is expected to be strongly modulated by the chemical–physical conditions at which measurements are performed, such as temperature, pH, ionic strength, *etc*. On the other hand, since AFS experiments are performed in non-equilibrium under the application of an external force, the measured unbinding force varies with the loading rate that the biomolecules feel when they are pulled apart, as widely discussed in the next section. To get an idea about the range spanned by the unbinding forces are placed, a list of the values for some representative biomolecular complexes is reported in Table 1; the nominal loading rate at which the corresponding measurement has been performed being also reported. For an almost exhaustive list of complexes investigated by AFS see *e.g*. refs. 33 and 125. At the loading rate of 10 nN s^{-1}, the unbinding force values have been found in a rather wide range, from 20 up to 240 pN. Strong and

Table 1 Unbinding force and the dissociation rate k_{off} for some ligand–receptor pairs; the measured loading rate at the unbinding force is also reported. Multiple k_{off} values refer to different fits of two different linear trends

Complex	Unbinding force/pN	Loading rate/nN s^{-1}	k_{off}/s^{-1}	Ref.
αβ integrin–GRGDSP peptide	20 ± 7	10	0.13, 59 ± 7	115
Cadherin–cadherin	35 ± 16	10	~1.8	37
p53/mdm2	105 ± 6	3	~1.5	117
H Serum albumin–anti H serum albumin	244 ± 22	10		113
Antilysozyme Fv fragment–lysozyme	55 ± 10	10	0.001, 150	97
Mucin1–antibody	120	10	$\sim 2.6 \times 10^{-3}$	34
Fv of fluorescein binding antibody–fluorescein antigen	160 ± 15	10	0.062	35
Azurin–cytocrome c551	95 ± 1	10	~6–14	38, 83
p53–azurin	75 ± 15	10	~0.09	103
P-selectin–PSGL-1 ligand	115 ± 40	10		87
Carbonic anhydrase–sulfonamide inhibitor	65	10	0.8–3.4	133
Thrombin–aptamer	4.5	3		114
PDZ Domain–recognition peptide	120	10	0.03, 11	135
Biotin–avidin	50	1	10	122
Biotin–avidin	130	1	$\sim 6.5 \times 10^{-6}$, 0.08	112
Biotin–streptavidin	150	1	$\sim 1.7 \times 10^{-5}$, 2.09	112
Biotin–streptavidin	55	1	23 ± 16	60

highly specific biomolecular interactions, such as antigen–antibody complexes, generally are characterized by higher values, while complexes with a "weak character" show lower force values. However, a direct correlation between the unbinding force value and the character of the interaction cannot be established. In this connection, it is interesting to note that a rather high unbinding force, around 100 pN, has been measured for the electron transfer complex between azurin and cytochrome c551; the transient character of such a complex making this result particularly intriguing.[38,83]

Perhaps significantly, some variability in the unbinding force value has been observed when complexes with similar biological functions are analyzed, *e.g.* for antigen/antibody pairs. On the other hand, a particular attention has been devoted to the biotin–avidin pair, or closely related complexes, such as biotin–streptavidin, biotin–neutravidin pairs, which are characterized by a strong affinity, and representing a kind of benchmark for investigating the properties of biomolecular complexes. Indeed, the study of these complexes, under different conditions and by different research groups, has put into evidence a rather large variability in the measured unbinding force.[12,29,77,107,122,126–129] For biotin–avidin, at a loading rate of 1 nN s^{-1}, unbinding forces values from 50 to 170 pN have been obtained, while for biotin-streptavidin, values from 55 to 150 pN have been measured (see Table 1).[60,107,122] A similar variability in the unbinding force values has been also observed in the experiments performed using a biomembrane force probe.[41,130] These discrepancies have stimulated a revisitation of their unbinding process in the light of the biomolecular complexity, involving an energy landscape characterized by many nearly isoenergetic local minima.[60,131] During the binding and unbinding processes, the partners can explore multiple energetic barriers which give rise to a huge variety of possible unbinding paths, and then to a spread of the unbinding force values.[60] Measurements performed at different temperatures, and even for long times, allow to reach a complete relaxation of the system, making possible to reconstruct the full energy landscape, and avoiding discrepancies among experiments.[41,132] Therefore, the recent development of extremely stable AFM apparata characterized by very low drift could be useful to study the unbinding processes for long times.[132]

6. Models to analyze AFS data

6.1 Bell–Evans model

As already mentioned, the application of an external force to a biomolecular complex drastically alters the energy profile of the unbinding process, hence AFS measurements are performed in non-equilibrium conditions. Development of suitable models to extract information on the equilibrium properties from non-equilibrium conditions has required large efforts.

A phenomenological description of the effects of an applied force on the energy profile of a reaction has been first provided by Bell to describe cell-to-cell adhesion.[30] According to him, a forced dissociation can be described as a thermally activated reaction in the framework of the reaction rate theory. More specifically, using the Boltzmann *Ansatz*, Bell predicted a decrease of the activation free energy for a reaction at zero force, $\Delta G^*(0)$, by a factor proportional to the applied force F: $\Delta G^*(F) = \Delta G^*(0) - Fx_\beta$; where $\Delta G^*(F)$ is the activation free energy under the application of a force F, x_β is the reaction coordinate corresponding to the separation between the bound and the transition state, projected along the direction of the applied force (see Fig. 1); x_β is assumed to be not affected by the force.[30] Accordingly, the dissociation rate $k_{off}(F)$, for an unbinding process under the application of a force F, increases exponentially:

$$k_{off}(F) = k_{off} \exp(Fx_\beta/k_B T) \quad (4)$$

where k_{off} is the dissociation rate at zero force (at equilibrium condition $k_{off} = k_{off}(0)$). Consistently, the lifetime of the complex, given by $\tau_{off}(F) = 1/k_{off}(F)$ is shortened with respect to that of a spontaneous dissociation. Due to this change in timescale, even slow dissociation processes could become accessible to the temporal resolution of AFS, which ranges from milliseconds to seconds.

Evans and Ritchie, starting from the Bell's assumption, derived a description of the unbinding process in terms of a crossing over a single, sharp barrier through the application of a time-dependent force $F(t)$, providing thus the dependence of the unbinding force on the loading rate.[30,31] Such a phenomenological model, commonly named the Bell–Evans model,[133] is based on a series of commonly accepted assumptions: (i) the loading rate during a measurement is constant, and then the force increases linearly with time, *i.e.* $F = Rt$; (ii) a single couple of interacting biomolecules is investigated during the process; (iii) the rupture time is longer than the diffusional relaxation time and the occurrence of a rebinding process is neglected; (iv) the pulling coordinate is implicitely assumed to coincide with the reaction coordinate.

On such a basis, the survival probability $S(t)$ of the process, *i.e.* the probability that the unbinding has not yet occurred at the time t, has to satisfy the first-order rate equation with a time-dependent dissociation rate $k_{off}(F(t))$:

$$dS(t)/dt = -k_{off}(F(t))S(t) \quad (5)$$

and thus:

$$S(t) = \exp[-\int_0^t k_{off}(t')\,dt'] \quad (6)$$

$S(t)$ is connected to the unbinding force probability distribution $P(F)$ by: $P(F)\,dF = -\dot{S}(\tau)\,d\tau$ where τ is the lifetime of the complex. Then, the probability distribution $P(F)$ is:[40]

$$P(F) = \frac{k_{off}(F)}{R}\exp\left[-\int_0^F \frac{k_{off}(F')}{R(F')}dF'\right] \quad (7)$$

where the relationship $dF = Rdt$ has been used. By introducing the Bell's assumption, and carrying on the integration in eqn (7), $P(F)$ becomes:

$$P(F) = \frac{k_{off}}{R}\exp\left[\frac{Fx_\beta}{k_BT} + \frac{k_{off}k_BT}{x_\beta R}\left(1-\exp\left(\frac{Fx_\beta}{k_BT}\right)\right)\right] \quad (8)$$

This distribution is asymmetric and skewed towards low force values.[41,89,134] Notably, the real unbinding force distributions often show an opposite trend with a skew towards high forces. Such a behaviour could be due to the contribution to the unbinding forces arising from other effects, such as different binding sites, multiple events, binding heterogeneity, as already mentioned.[34,119] The most probable unbinding force, F^*, at a fixed value of the loading rate, can be then obtained by calculating the maximum of the $P(F)$ distribution, which is given by eqn (8):[31]

$$F^* = \frac{k_BT}{x_\beta}\ln\left(\frac{Rx_\beta}{k_{off}k_BT}\right) \quad (9)$$

Eqn (9) puts into relationship the most probable force F^*, at a given loading rate, with the dissociation rate at zero force, k_{off}, and the position of the energy barrier along the reaction coordinate, x_β (see Fig. 1). More specifically, it predicts a linear relationship between the most probable force F^*, with the logarithm of the loading rate. Therefore, by measuring the most probable unbinding force as a function of loading rate and plotting F^* *vs.* ln R, k_{off} and x_β can be extracted from the slope and intercept, respectively, of the fitting linear curve.

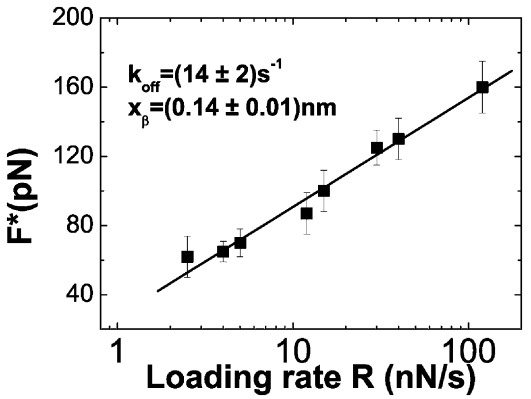

Fig. 8 An example of a linear dependence of the loading-rate on the most probable unbinding force F^*. The solid line is a numerical fit of experimental data to the Bell–Evans model (see eqn (9)) (data from ref. 38). Best-fitting parameters are shown.

The modality in which AFS measurements are done by varying the loading rate, is commonly termed dynamic force spectroscopy (DFS). DFS experiments are commonly performed by changing the retraction speed, while keeping the approach speed constant;[35] the former being usually varied in the 0.1–100 nN s^{-1} range.[16]

The Bell–Evans model has provided a good description of the unbinding force as a function of the loading rate for several biomolecular complexes.

An example of a linear dependence for the measured most probable force unbinding, with the loading rate (varying between 1–100 nN s^{-1}), is shown in Fig. 8; the extracted k_{off} and x_β values by a fit through eqn (9) being also reported.

In Table 1, the k_{off} values taken from literature for some representative pairs of biomolecules are reported. Generally, the k_{off} rates vary in a very wide range, from 10^{-6} to 150 s^{-1}; such a variability being indicative that the kinetic properties of biological complexes, at single molecule level, are characterized by very different timescales. Remarkably, the k_{off} values obtained by AFS can be compared with those derived from bulk techniques, such as SPR. In such a way, possible differences in unbinding properties of interacting biomolecules from those of bulk can be put into evidence.[34,97,103]

As discussed in section 2, the dissociation rate k_{off} is connected to the specificity of a biorecognition reaction. Hence, its estimation, at single molecule level, constitutes an important piece of information to elucidate the mechanisms underlying the biorecognition processes.

For some systems, two different values of k_{off} are reported in Table 1. In these cases, the most probable unbinding force as a function of the loading rate exhibits two distinct linear regimes, and then two k_{off} values have been extracted by two independent linear fits. Such a behavior can be traced back to the presence of two intermediate states in the unbinding process, instead of a single barrier (see Fig. 9A and B).[60,88]

The presence of multiple barriers in the energy landscape commonly emerges when unbinding processes are investigated in a wider range of loading rates, and especially when the analysis is extended to low loading rates.[112,122,135] These studies are becoming more and more accessible thanks to the development of AFM equipments with a high stability in time.

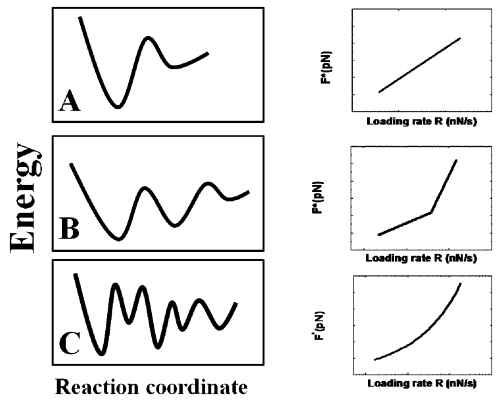

Fig. 9 Left: schematic diagrams of the energy profile for a dissociation process of a biomolecular complex. Right: the corresponding trend for most probable unbinding force F^* as a function of the loading rate.

From the study of the interaction between biomolecules by AFS, the association rate k_{on}, and then the association constant, $K_a = k_{on}/k_{off}$, indicative of the affinity, can be also derived. A rough estimation of the k_{on} rate can be obtained by following the procedure proposed in ref. 28. Accordingly, k_{on} can be given by $k_{on} = N_A V_{eff}/t_{0.5}$, where N_A is the Avogadro's number, V_{eff} is the effective volume of a half-sphere, with radius r_{eff} around the tip, which allows the biomolecule to bind to the partner, and $t_{0.5}$ is the time required for the half-maximal binding probability; $t_{0.5}$ being $2r_{eff}/v$ where v is the approach speed of the cantilever. Therefore, upon determining k_{off} and k_{on}, the association constant, $K_a = k_{on}/k_{off}$, can be evaluated in single molecule regime and compared with that obtained in bulk by other techniques. Notably, the equilibrium activation free energy, ΔG, can be also calculated from eqn (2) by a van't Hoff plot of the logarithm of k_{off} *vs.* $1/T$.

6.2 Revisions of the Bell–Evans model

Although the Bell–Evans model has allowed to successfully describe the trend of the most probable unbinding force with the loading rate for several biomolecular complexes, deviations from the linear trend, such as that schematically represented in Fig. 9C (right), have been observed in some cases.[39,40,115] Furthermore, some discrepancies have been registered in the k_{off} values, as evaluated for the same system.[60] All these aspects have led to search a more consistent and general picture of the unbinding force trend as a function of the loading rate, by developing new theoretical approaches or by revisiting the Bell–Evans model.

General treatments of the unbinding processes for interacting biomolecules have been proposed in the framework of the Kramers theory of thermally activated barrier crossing by assuming an analytical expression for the barrier potential in the presence of an applied force.[42,136] Hummer and Szabo have proposed a harmonic free energy surface with a single sharp barrier described by a cusp surface.[40] They found that, at intermediate pulling speeds, the most probable unbinding force follows a trend with the logarithm of the loading rate such as: $F^* \sim (\ln R)^{1/2}$. We note that such a model reduces to the Bell–Evans one if the free energy barrier is very large ($\Delta G \rightarrow \infty$).

Alternatively, Dudko *et al.* have derived a model by assuming a linear–cubic expression for the free energy surface.[39] They found that, for high forces, the distribution of the unbinding forces is asymmetric and that the most probable unbinding force follows the trend: $F^* \sim (\ln R)^{2/3}$. Remarkably, the models of Hummer and Szabo and of Dudko *et al.* have been recently cast into a common framework, also including the phenomenological approach of Bell–Evans.[42] Accordingly, the most probable unbinding force has been expressed as: $F^* \sim (\ln R)^{\nu}$ where ν can assume the value 1, 1/2 or 2/3 depending on which model better describes the behavior of the system.

On the other hand, the Bell–Evans model has been revisited in order to provide a more consistent description of the experimental data. In the following, the main aspects of the model, which have been object of revision, will be addressed.

(i) The Bell–Evans model assumes that the loading rate is constant during the measurements. The loading rate value has been first derived from the nominal loading rate obtained by the product of the spring constant and the retraction speed.[87–88,112] Such an approximation is valid if the load on the complex increases sufficiently slowly, so that there is time for thermal fluctuations to drive the system over the energy barrier.[32] More appropriately, to take into account for the contribution to the loading rate of the molecular stretching, the nominal loading rate has to be replaced with the instantaneous loading rate provided by the slope of the tether extension curve close to the rupture event (see Fig. 5).[35,108] However, the very low reproducibility of the AFS data, especially when polymer linkers are used, has led to question the assumption that the loading rate is constant during the measurements. Indeed, flexible polymer linkers, which are formed by highly nonlinear springs, may undergo a stretching with a variable path, yielding some changes in the loading rate values from curve to curve.[35] Accordingly, it has been suggested to estimate the apparent loading rate by averaging the measured effective spring constant over a collection of force curves (at least ten) obtained at the same probe speed.[137] Moreover, an analytical model which corrects the systematic errors arising from polymer tether elasticity, has been recently proposed.[138]

(ii) One mandatory requirement of the Bell–Evans model is that the unbinding experiment is performed on a single couple of interacting biomolecules. However, the unbinding events might involve more than one pair. An extension of the model to take into account for multiple unbinding has been developed in terms of a Markovian sequence. In particular, under the assumption that n bonds between several identical couples in parallel break simultaneously in a uncorrelated way, eqn (9) has been replaced by the following expression:[139]

$$\frac{1}{R} = \frac{x_\beta}{k_{off} k_B T} \sum_{l=1}^{n} \frac{1}{l} \exp\left(-\frac{F^* x_\beta}{l k_B T}\right) \qquad (10)$$

This provides a relationship between the most probable rupture force F^* and the effective loading rate R, which is given by $1/n$ of the nominal loading rate, since it is shared among the n bonds.[120] The application of eqn (10), however, requires some iterative processes to determine the effective number of interacting pairs.[34]

(iii) The Bell–Evans model assumes that during the measurements, the rebinding between the two partners is negligible. Indeed, if measurements are performed at sufficiently slow rates, some relaxation and rebinding process could take place. Actually, in near-equilibrium processes, rebindings do occur and the unbinding force becomes almost independent on the loading rate.[136] On the other hand, measurements in the slow regime offer the possibility to extract information on the free energy change which are not accessible to standard AFS experiments. Recent theoretical works have provided a quantitative description of the influence of a finite rebinding probability on the unbinding process under the effect of an external force; this leading to a new piece of information on the systems at equilibrium.[140,141]

(iv) Finally, a method, based on a generalization of the Bell–Evans approach to directly determine the force-dependent lifetime $\tau(F)$ from the rupture force histograms. has been developed. [142] Such an approach has the advantage to maintain some validity even when the pulling coordinate does not coincide with the reaction coordinate.

6.3 Free energy estimation by the Jarzynski identity

The knowledge of the equilibrium free energy, ΔG, which gives the difference between the free and bound state of a reaction, is of utmost importance for understanding the properties of a biorecognition process. For an unbinding process of two interacting biomolecules, ΔG is related to the association constant, K_a, through the expression:

$$K_a = \exp(\Delta G/RT) \qquad (11)$$

In principle, the evaluation of ΔG requires the accessibility of the equilibrium regime together with a complete sampling of the configurational space.[143,144] However, many experiments, including AFS, are performed in non-equilibrium conditions.

Recently, a theoretical model allowing a direct evaluation of the free energy difference, ΔG, from non-equilibrium experiments, has been developed by Jarzynski.[43] The main result is summarized by the Jarzynski identity (JI):

$$\exp(-\Delta G/k_B T) = \int \rho(W_\lambda) \exp(-W_\lambda/k_B T)\, dW_\lambda \qquad (12)$$

where W_λ is the mechanical work done along the non-equilibrium path λ and $\rho(W_\lambda)$ is the non-equilibrium work distribution. The work can be calculated by: $W_\lambda = \int F d\lambda$ where F is the external force applied to the system. Generally, application of eqn (12) requires that multiple measurements of W_λ at a sufficiently high signal/noise ratio are available.

Although the JI is formally simple, its application to single molecule experimental data can present some difficulties from both the theoretical and experimental points of view; for a discussion on these aspects, see refs. 143 and 145. In particular, it is of utmost importance that the multiple measurements are performed exactly under the same conditions [146] and this requires that the employed AFM equipment is very stable in time.

Starting from the Hummer and Szabo remodelling of the JI to the analysis of single molecule experiments,[146] the JI has been then applied to reconstruct the free energy landscape of the irreversible unfolding of molecules.[143,147,148]

Very recently, the JI has been applied to the study by AFS of the unbinding process of a biological complex.[149] To calculate the equilibrium free energy difference, ΔG, the following expression has been used:

$$\exp(-\Delta G/k_B T) = \sum_{i=1}^{N} \frac{1}{N} \exp(-W_i/k_B T) \qquad (13)$$

where N is the number of independent repetitions of the process, W_i is the work done from the applied force and the corresponding extension of the molecular system along a particular path. Notably, eqn (13) is equivalent to eqn (12) for $N \to \infty$. In practice since the limited number of experiments, the standard deviation of the work should be not greater than $k_B T$ and the measurement errors should be kept sufficiently low over a rather large number of trajectories.[143] Furthermore, the pulling apparatus should be equilibrated at a fixed, initial position in all the trajectories.[147] The application of the JI to evaluate the free energy of unbinding processes deserves significant interest as it provides capabilities for a deep investigation of biological complexes at single molecule level.

7. Summary and future perspectives

In the last few years, the study of the mechanisms which govern the interactions between biomolecules has received new impetus from the application of single molecule spectroscopies. While in conventional ensemble experiments, large numbers of biomolecules are interrogated simultaneously and average properties are extracted, in single molecule experiments molecules are probed one at a time, gaining access to an incredible wealth of information.

AFS represents one of the most rewarding tools for studying biological recognition processes, allowing to measure forces acting between individual biomolecules with a pN sensitivity, in near-physiological conditions and without labelling. Furthermore, AFS experiments provide information on the dissociation rate, k_{off}, and on the activation free energy for a single couple of interacting biomolecules, complementing traditional biochemical approaches.

AFS is part of the technologically advanced family of scanning probe microscopies (AFM, conductive-AFM, STM, *etc.*), which are progressively becoming more appreciated in the biophysical and biological community, and are widely applied to study a large number of biomolecular complexes. AFS has also demonstrated enormous capabilities for investigating non-conventional aspects of biorecognition processes, averaged-out in the ensemble studies, such as rare events, influence of local environmental changes, molecular crowding, molecular heterogeneity, conformational changes, *etc*. Furthermore, it allows to clarify how the biorecognition ability of biomolecules, and their kinetic response, are modified when they undergo a diffusional restriction upon immobilization on a surface. In this respect, the combination of AFS with the SPR bulk technique could be very fruitful to gain further complementary information on biomolecular specific interactions.

The occurrence of some controversial and ambiguous AFS results from new biological complexes, or from paradigmatic,

well-investigated systems, such as biotin–avidin, has led to revisitation of some experimental and theoretical aspects of AFS. Among these, three main crucial points deserving particular attention, have been outlined. First, the requirement of sampling only one pair of biomolecules during AFS experiments, should be satisfied, at the best, to avoid complications in the data analysis. Accordingly, large efforts have been devoted to develop immobilization strategies which are able to drastically reduce the probability that more than one pair of interacting biomolecules is investigated. Even if a definite strategy, suitable for all the systems, has not been implemented, a collection of several, widely-tested strategies are now available to be adapted to the system under analysis. Second, a special care should be paid to reliably discriminate between specific and nonspecific unbinding events. This task can be fulfilled, at the best, by performing a deep analysis of the force curve cycles, with a particular attention to the properties of the curve immediately before the jump-off-contact. Such an analysis is greatly facilitated by the use of suitable flexible linkers connecting the inorganic surfaces with the biomolecules, and undergoing a controlled stretching during the unbinding process. In this respect, automatic procedures to analyze the large amount of force curves of an AFS experiment have started to be implemented, promoting, in this way, AFS as a routine approach in research laboratories.

Third, a more reliable description of the non-equilibrium force-driven AFS data is required in order to gain a deeper insight on the equilibrium parameters. In this connection, the application of new theoretical tools, such the Jarzynski identity, for analyzing unbinding processes appears to be very promising to reach a full description of the energy landscape of the biological systems. Furthermore, the complexity of the energy landscape of biomolecules, characterized by many isoenergetic local minima, should be taken into account to yield a consistent description of biorecognition processes.

It can be easily predicted that AFS will undergo significant improvements and developments in the near future. The quite recent introduction of low-drift AFM apparata could lead to significant advances in AFS experiments, making possible to perform measurements for long times, and then to follow processes at near-equilibrium.[132] At the same time new high speed AFM equipment makes it possible to monitor fast biological events in real time.[150]

Moreover, the coupling of AFS with other single-molecule techniques is very promising to provide, in perspective, a deeper description of the biorecognition processes. On the other hand, the combination of AFS with high-resolution AFM imaging could offer the possibility to get insights into the interplay between structure and functionality.

Finally, AFS can also be a valuable tool for applications in nanotechnology through the coupling of single molecule manipulation with the detection of mechanical, chemical and electrical effects for the developments of innovative nanodevices, such as molecular motors, biosensors, *etc*. In particular, AFS has demonstrated to display high potentialities in nano-biodiagnostics especially in combination with ultra-sensitive optical spectroscopies, such as advanced fluorescence.[25] Furthermore, force detection combined with measurements by STM or conductive-AFM, by employing conductive substrates (*e.g*. gold, graphite or even nanotubes), could be an optimal starting point for advanced applications in innovative biosensors.

Notes and references

1 M. Wilchek, E. A. Bayer and O. Livnah, *Immunol. Lett*., 2006, **103**, 27.
2 D. A. Lauffenburger and J. J. Linferman, *Receptors: Models for Binding, Trafficking and Signaling*, Oxford University Press, New York, 1993.
3 D. Morikis and J. D. Lambris, *Trends Immunol*., 2004, **25**, 700.
4 R. B. Lindorff-Larsen, M. A. Best, M. A. De Pristo, C. M. Dobson and M. Vendruscolo, *Nature*, 2005, **433**, 128.
5 P. Schuck, *Annu. Rev. Biophys. Biomol. Struct*., 1997, **26**, 541.
6 K. C. Neuman and A. Nagy, *Nat. Methods*, 2008, **5**, 491.
7 A. Deniz, S. Mukhopadhyay and E. A. Lemke, *J. R. Soc. Interface*, 2008, **5**, 15.
8 H. Miyata, R. Yasuda and K. Kinosita, Jr., *Biochim. Biophys. Res. Commun*., 1996, **1290**, 83.
9 E. Evans, K. Ritchie and R. Merkel, *Biophys. J*., 1995, **68**, 2580.
10 G. Kaplanski, C. Farnarier, O. Tissot, A. Pierres, A. M. Benoliel, M. C. Alessi, S. Kaplanski and P. Bongrand, *Biophys. J*., 1993, **64**, 1922.
11 R. D. Alon, A. Hammer and T. A. Springer, *Nature*, 1995, **374**, 539.
12 E. L. Florin, V. T. Moy and H. E. Gaub, *Science*, 1994, **264**, 415.
13 P. L. Frederix, T. Akiyama, U. Staufer, C. Gerber, D. Fotiadis, D. J. Muller and A. Engel, *Curr. Opin. Chem. Biol*., 2003, **7**, 641.
14 J. B. P. Jena and J. K. Hoerner, *Atomic Force Microscopy in Cell Biology, Methods in Cell Biology*, Academic Press, San Diego, CA, 2002, vol. 68.
15 H. J. Butt, B. Cappella and M. Kappl, *Surf. Sci. Rep*., 2005, **59**, 1.
16 P. Hinterdorfer and Y. F. Dufrene, *Nat. Methods*, 2006, **3**, 347.
17 P. E. Marszalek, H. Lu, H. Li, M. Carrion-Vazquez, A. F. Oberhauser, K. Schulten and J. M. Fernandez, *Nature*, 1999, **402**, 100.
18 R. Lavery, A. Lebrun, J. F. Allemand, D. Bensimon and V. Croquette, *J. Phys.: Condens. Matter*, 2002, **14**, R383.
19 M. Rief, M. Gautel, F. Oesterhelt, J. M. Fernandez and H. E. Gaub, *Science*, 1997, **276**, 1109.
20 D. J. Muller, W. Baumeister and A. Engel, *Proc. Natl. Acad. Sci. U. S. A*., 1999, **96**, 13170.
21 F. Oesterhelt, M. Rief and H. E. Gaub, *New J. Phys*., 1999, **1**, 6.
22 A. F. Oberhauser, P. K. Hansma, M. Carrion-Vazquez and J. M. Fernandez, *Proc. Natl. Acad. Sci. U. S. A*., 2001, **98**, 468.
23 S. E. Cross, Y. S. Jin, J. Rao and J. K. Gimzewski, *Nat. Methods*, 2007, **2**, 780.
24 K. Blank, T. Mai, I. Gilbert, S. Schiffmann, J. Rankl, R. Zivin, C. Tackney, T. Nicolaus, K. Spinnler, F. Oesterhelt, M. Benoit, H. Clausen-Schaumann and H. E. Gaub, *Proc. Natl. Acad. Sci. U. S. A*., 2003, **100**, 11356.
25 A. K. Sinensky and A. M. Belcher, *Nat. Methods*, 2007, **2**, 253.
26 B. Bonanni, L. Andolfi, A. R. Bizzarri and S. Cannistraro, *J. Phys. Chem. B*, 2007, **111**, 5062.
27 J. Baudry, E. Bertrand, N. Lequeeux and J. Bibette, *J. Phys.: Condens. Matter*, 2004, **14**, R383.
28 P. Hinterdorfer, W. Baumgartner, H. J. Gruber, K. Schilcher and H. Schindler, *Proc. Natl. Acad. Sci. U. S. A*., 1996, **93**, 3477.
29 G. U. Lee, D. A. Kidwell and R. J. Colton, *Langmuir*, 1994, **10**, 354.
30 G. I. Bell, *Science*, 1978, **200**, 618.
31 E. Evans and K. Ritchie, *Biophys. J*., 1997, **72**, 1541.
32 E. Evans, *Annu. Rev. Biophys. Biomol. Struct*., 2001, **30**, 105.
33 C. K. Lee, Y. M. Wang, L. S. Huang and S. Lin, *Micron*, 2007, **38**, 446.
34 T. A. Sulchek, R. W. Friddle, K. Langry, E. Y. Lau, H. Albrecht, T. V. Ratto, S. J. DeNardo, M. E. Colvin and A. Noy, *Proc. Natl. Acad. Sci. U. S. A*., 2005, **102**, 16638.
35 F. Schwesinger, R. Ros, T. Strunz, D. Anselmetti, H. J. Guntherodt, A. Honegger, L. Jermutus, A. L. Tiefenauer and A. Pluckthun, *Proc. Natl. Acad. Sci. U. S. A*., 2000, **97**, 9972.

36 O. H. Willemsen, M. E. Snel, A. Cambi, J. Greve, B. G. De Grooth and C. G. Figdor, *Biophys. J.*, 2000, **79**, 3267.
37 W. Baumgartner, P. Hinterdorfer, W. Ness, A. Raab, D. Vestweber, H. Schindler and D. Drenckhahn, *Proc. Natl. Acad. Sci. U. S. A.*, 2000, **97**, 4005.
38 B. Bonanni, A. S. M. Kamruzzahan, A. R. Bizzarri, C. Rankl, H. J. Gruber, P. Hinterdorfer and S. Cannistraro, *Biophys. J.*, 2005, **89**, 2783.
39 O. K. Dudko, A. E. Filippov, J. Klafter and M. Urbakh, *Proc. Natl. Acad. Sci. U. S. A.*, 2003, **100**, 11378.
40 G. Hummer and A. Szabo, *Biophys. J.*, 2003, **85**, 5.
41 F. Pincet and J. Husson, *Biophys. J.*, 2005, **89**, 4374.
42 O. K. Dudko, G. Hummer and A. Szabo, *Phys. Rev. Lett.*, 2006, **96**, 108101.
43 C. Jarzynski, *Phys. Rev. Lett.*, 1997, **78**, 2690.
44 J. Janin, *Prog. Biophys. Mol. Biol.*, 1995, **64**, 145.
45 M. Prudêncio and M. Ubbink, *J. Mol. Recognit.*, 2004, **17**, 524.
46 A. R. Bizzarri, E. Brunori, B. Bonanni and S. Cannistraro, *J. Mol. Recognit.*, 2007, **20**, 122.
47 S. Jones and J. M. Thornton, *Proc. Natl. Acad. Sci. U. S. A.*, 1996, **93**, 13.
48 S. Vajda and C. J. Camacho, *Trends Biotechnol.*, 2004, **22**, 110.
49 D. K. Koshland, *Angew. Chem., Int. Ed. Engl.*, 1995, **33**, 2375.
50 B. L. Stoddard and D. E. Koshland, *Nature*, 1992, **358**, 774.
51 O. F. Lange, N. A. Lakomek, C. Farès, G. F. Schröder, K. F. A. Walter, S. Becker, J. Meiler, H. Grubmüller, C. Griesinger and B. L. de Groot, *Science*, 2008, **320**, 1471.
52 P. Robert, A. M. Benoliel, A. Pierres and P. Bongrand, *J. Mol. Recognit.*, 2007, **20**, 432.
53 H. A. Kramers, *Physica*, 1940, **7**, 284.
54 J. Foote and C. Milstein, *Nature*, 1991, **352**, 530.
55 K. Matsui, J. J. Boniface, P. Steffner, P. A. Reay and M. M. Davis, *Proc. Natl. Acad. Sci. U. S. A.*, 1994, **91**, 12862.
56 A. Pierres, A. M. Benoliel, C. Zhu and P. C. Bongrand, *Biophys. J.*, 2001, **81**, 25.
57 C. Jeppesen, J. Y. Wong, T. L. Kuhl, J. N. Israelachvili, N. Mullah and S. Zalipsky, *Science*, 2001, **293**, 465.
58 J. Homola, *Anal. Bioanal. Chem.*, 2003, **377**, 528.
59 P. Nassoy, *Biophys. J.*, 2007, **93**, 361.
60 F. Rico and V. T. Moy, *J. Mol. Recognit.*, 2007, **20**, 495.
61 G. Binnig, C. F. G. Quate and C. F. Gerber, *Phys. Rev. Lett.*, 1986, **56**, 930.
62 E. Meyer, H. Heinzelmann, P. Gruetter, T. Jung, T. Weisskopf, H. R. Hidber, R. Lapka, H. Rudin and H. J. Guentherodt, *J. Microsc.*, 1988, **152**, 269.
63 S. Alexander, L. Hellemans, O. Marti, J. Schneir, V. Elings, P. K. Hansma, M. Longmire and J. Gurley, *J. Appl. Phys.*, 1989, **65**, 164.
64 Q. Zhong, D. Innis, K. Kjoller and V. B. Elings, *Surf. Sci.*, 1993, **290**, L688.
65 J. K. Horber and M. J. Miles, *Science*, 2003, **302**, 1002.
66 Y. Seo and W. Jhe, *Rep. Prog. Phys.*, 2008, **71**, 016101–1.
67 D. J. Müller and Y. F. Dufrêne, *Nat. Nanotechnol.*, 2008, **3**, 261.
68 S. R. Cohen and A. Bitler, *Curr. Opin. Colloid Interface Sci.*, 2008, **13**, 316.
69 P. J. Cumpson, P. Zhdan and J. Hedley, *Ultramicroscopy*, 2004, **100**, 241.
70 J. P. Cleveland, S. Manne, D. Bocek and P. K. Hansma, *Rev. Sci. Instrum.*, 1993, **64**, 403.
71 J. L. Hutter and J. Bechhoefer, *Rev. Sci. Instrum.*, 1993, **64**, 1868.
72 M. B. Viani, T. E. Schäffer, G. T. Paloczi, L. I. Pietrasanta, B. L. Smith, J. B. Thompson, M. Richter, M. Rief and H. E. Gaub, *Rev. Sci. Instrum.*, 1999, **70**, 4300.
73 R. V. Lapshin, *Rev. Sci. Instrum.*, 1995, **66**, 4718.
74 M. Radmacher, M. Fritz, H. G. Hansma and P. K. Hansma, *Science*, 1994, **265**, 1577.
75 A. Engel and D. J. Mueller, *Nat. Struct. Biol.*, 2000, **7**, 715.
76 J. Wong, A. Chilkoti and V. T. Moy, *Biomol. Eng.*, 1999, **16**, 45.
77 V. T. Moy, E. L. Florin and H. E. Gaub, *Science*, 1994, **266**, 257.
78 A. Ulman, *Chem. Rev.*, 1996, **96**, 1533.
79 B. Bonanni, D. Alliata, A. R. Bizzarri and S. Cannistraro, *ChemPhysChem*, 2003, **4**, 1183.
80 L. Andolfi, A. R. Bizzarri and S. Cannistraro, *Appl. Phys. Lett.*, 2006, **89**, 183125.
81 U. Dammer, O. Popescu, P. Wagner, D. Anselmetti, H. J. Guentherodt and G. N. Misevic, *Science*, 1995, **267**, 1173.
82 J. J. Davis and H. A. O. Hill, *Chem. Commun.*, 2002, 393.
83 B. Bonanni, A. R. Bizzarri and S. Cannistraro, *J. Phys. Chem. B*, 2006, **110**, 14574.
84 T. V. Ratto, K. C. Langry, R. E. Rudd, R. Balhorn and M. McElfresh, *Biophys. J.*, 2004, **86**, 2430.
85 O. H. Willemsen, M. M. Snel, K. O. van der Werfs, B. G. de Grooth, J. Greve, P. Hinterdorfer, H. J. Gruber, H. Schindler, Y. van Kooyk and C. G. Y. Figdor, *Biophys. J.*, 1998, **75**, 2220.
86 T. Haselgruebler, A. Amerstorfer, H. Schndler and H. Gruber, *Bioconjugate Chem.*, 1995, **6**, 242.
87 J. Fritz, A. G. Katopodis, F. Kolbinger and D. Anselmetti, *Proc. Natl. Acad. Sci. U. S. A.*, 1998, **95**, 12283.
88 T. K. Strunz, K. Oroszlan, R. Schaefer and H. J. Guentherodt, *Proc. Natl. Acad. Sci. U. S. A.*, 1999, **96**, 11277.
89 J. Morfill, K. Blank, C. Zahnd, B. Luginbuhl, F. Kuhner, K. E. Gottschalk, A. Pluckthun and H. E. Gaub, *Biophys. J.*, 2007, **93**, 3583.
90 L. A. Chtcheglova, G. T. Shubeita, S. K. Sekatskii and G. Dietler, *Biophys. J.*, 2004, **86**, 1177.
91 P. Wagner, *FEBS Lett.*, 1998, **430**, 112.
92 M. Rief, M. Gautel, A. Schemmel and H. E. Gaub, *Biophys. J.*, 1998, **75**, 3008.
93 R. Yasuda, H. Noji, K. Kinosita, Jr. and M. Yoshida, *Cell*, 1998, **93**, 1117.
94 C. Verbelen, H. J. Gruber and Y. F. Dufrene, *J. Mol. Recognit.*, 2007, **20**, 490.
95 R. Ros, F. Schwesinger, D. Anselmetti, M. Kubon, R. Schaefer, A. Plueckuthun and L. Tiefenauer, *Proc. Natl. Acad. Sci. U. S. A.*, 1998, **95**, 7402.
96 F. Kienberger, G. Kada, H. J. Gruber, V. Pastushenko, C. Riener, M. Trieb, H.-G. Knaus, H. Schindler and P. Hinterdorfer, *Single Mol.*, 2000, **1**, 59.
97 A. Berquand, N. Xia, D. G. Castner, B. H. Clare, N. L. Abbott, V. Dupres, Y. Adriaensen and Y. F. Dufrêne, *Langmuir*, 2005, **21**, 5517.
98 E. Katz and I. Willner, *ChemPhysChem*, 2004, **5**, 1084.
99 Y. Gilbert, M. Deghorain, L. Wang, B. Xu, P. D. Pollheimer, H. J. Gruber, J. Errington, B. Hallet, X. Haulot, C. Verbelen, P. Hols and Y. F. Dufrêne, *Nano Lett.*, 2007, **7**, 796.
100 V. K. Yadavalli, J. G. Forbes and K. Wang, *Langmuir*, 2006, **22**, 6969.
101 T. A. Sulchek, R. Friddle and R. W. Noy, *Biophys. J.*, 2006, **90**, 4686.
102 A. R. Bizzarri, B. Bonanni and S. Cannistraro, *ChemPhysChem*, 2003, **4**, 1189.
103 M. Taranta, A. R. Bizzarri and S. Cannistraro, *J. Mol. Recognit.*, 2008, **21**, 63.
104 R. Chen and Z. Weng, *Proteins: Struct., Funct., Genet.*, 2002, **47**, 281.
105 V. De Grandis, A. R. Bizzarri and S. Cannistraro, *J. Mol. Recognit.*, 2007, **20**, 215.
106 M. Taranta, A. R. Bizzarri and S. Cannistraro, *J. Mol. Recognit.*, 2009, **22**, 215.
107 S. Allen, J. Davies, A. C. Dawkes, M. C. Davies, J. C. Edwards, M. C. Parker, C. J. Roberts, J. Sefton, S. J. B. Tendler and P. M. Williams, *FEBS Lett.*, 1996, **390**, 161.
108 C. Friedsam, A. K. Wehle, F. Kuhner and H. E. Gaub, *J. Phys.: Condens. Matter*, 2003, **15**, S1709.
109 M. Carrion-Vazquez, A. F. Oberhauser, T. E. Fisher, P. E. Marszalek, H. Li and J. M. Fernandez, *Prog. Biophys. Mol. Biol.*, 2000, **74**, 63.
110 W. Zhang and X. Zhang, *Prog. Polym. Sci.*, 2003, **28**, 1271.
111 F. Oesterhelt, D. Oesterhelt, M. Pfeiffer, A. Engel, H. E. Gaub and D. J. Mueller, *Science*, 2000, **288**, 143.
112 C. B. Yuan, A. Chen, P. Kolb and V. T. Moy, *Biochemistry*, 2000, **39**, 10219.
113 P. Hinterdorfer, F. Kienberger, A. Raab, H. J. Gruber, W. Baumgartner, G. Kada, C. Riener, S. Wielert-Badt, C. Borken and H. Schindler, *Single Mol.*, 2000, **1**, 99.
114 B. Basnar, R. Elnathan and I. Willner, *Anal. Chem.*, 2006, **78**, 3638.
115 X. H. Zhang, S. E. Craig, H. Kirby, M. J. Humphries and V. T. Moy, *Biophys. J.*, 2004, **87**, 3470.

116 M. Odorico, J. M. Teulon, O. Berthoumieu, S. W. Chen, P. Parot and J. L. Pellequer, *Ultramicroscopy*, 2007, **107**, 887.
117 G. Funari, F. Domenici, L. Nardinocchi, R. Puca, G. D'Orazi, A. R. Bizzarri and S. Cannistraro, *J. Mol. Recognit.*, in press.
118 C. R. Arciola, Y. Bustanji, M. Conti, D. Campoccia, L. Baldassarri, B. Samori' and L. Montanaro, *Biomaterials*, 2003, **24**, 3013.
119 F. Kienberger, A. Ebner, H. J. Gruber and P. Hinterdorfer, *Acc. Chem. Res.*, 2006, **39**, 29.
120 D. Hammer and S. Apte, *Biophys. J.*, 1992, **63**, 35.
121 A. B. Patel, S. Allen, M. C. Davies, C. J. Roberts, S. J. B. Tendler and P. M. Williams, *J. Am. Chem. Soc.*, 2004, **126**, 1318.
122 R. De Paris, T. Strunz, K. Oroszlan, H. J. Güntherodt and M. Hegner, *Single Mol.*, 2000, **1**, 285.
123 M. Odorico, J. M. Teulon, T. Bessou, C. Vidaud, L. Bellanger, S. W. Chen, F. Quemeneur, P. Parot and J. L. Pellequer, *Biophys. J.*, 2007, **93**, 645.
124 Fuhrmann, D. Anselmetti and R. Ros, *Phys. Rev. E: Stat., Nonlinear, Soft Matter Phys.*, 2008, **77**, 031912.
125 J. Zlatanova, S. M. J. Lindsay and S. H. Leuba, *Prog. Biophys. Mol. Biol.*, 2000, **74**, 37.
126 X. H. Zhang and V. T. Moy, *Biophys. Chem.*, 2003, **104**, 271.
127 Y. S. Lo, N. D. Huefner, W. S. Chan, F. Stevens, J. M. Harris and T. B. Beebe, Jr., *Langmuir*, 1999, **15**, 1373.
128 Y. S. Lo, Y. J. Zhu, Jr. and T. P. Beebe, Jr., *Langmuir*, 2001, **17**, 3741.
129 J. Zhou, L. Z. Zhang, Y. S. Leng, H. K. Tsao, Y. J. Sheng and S. J. Jiang, *J. Chem. Phys.*, 2006, **125**, 104905.
130 R. Merkel, P. Nassoy, A. Leung, K. Ritchie and E. Evans, *Nature*, 1999, **397**, 50.
131 H. Frauenfelder, F. Parak and R. D. Young, *Annu. Rev. Biophys. Chem.*, 1988, **17**, 451.
132 J. P. Junker, F. Ziegle and M. Rief, *Science*, 2009, **323**, 633.
133 G. Neuert, C. Albrecht, E. Pamir and H. E. Gaub, *FEBS Lett.*, 2006, **580**, 505.
134 M. Raible, M. Evstigneev, F. W. Bartels, R. Eckel, M. Nguyen-Duong, R. Merkel, R. Ros, D. Anselmetti and P. Reimann, *Biophys. J.*, 2006, **90**, 3851.
135 T. Maki, S. Kidoaki, K. Usui, H. Suzuki, M. Ito, F. Ito, Y. Hayashizaki and T. Matsuda, *Langmuir*, 2007, **23**, 2668.
136 R. W. Friddle, P. Podsiadlo, A. B. Artyukhin and A. Noy, *J. Phys. Chem. C*, 2008, **112**, 4986.
137 S. G. Kamper, L. Porter-Peden, R. Blankespoor, K. Sinniah, D. Zhou, C. Abell and T. Rayment, *Langmuir*, 2007, **23**, 12561.
138 C. Ray, J. R. Brown and B. B. Akhremitchev, *J. Phys. Chem. B*, 2007, **111**, 1963.
139 P. M. Williams, *Anal. Chim. Acta*, 2003, **479**, 107.
140 G. Diezemann and A. JanshoffJ, *J. Chem. Phys.*, 2008, **129**, 084904.
141 F. Li and D. Leckband, *J. Chem. Phys.*, 2006, **125**, 194702.
142 O. K. Dudko, G. Hummer and A. Szabo, *Proc. Natl. Acad. Sci. U. S. A.*, 2008, **105**, 15755.
143 J. Liphardt, S. Dumont, S. B. Smith, I. Tinoco and C. Bustamante, *Science*, 2002, **296**, 1832.
144 S. Park, F. Khalili-Araghi, E. Tajkhorshid and K. Schulten, *J. Chem. Phys.*, 2003, **119**, 3559.
145 G. Hummer and A. Szabo, *Acc. Chem. Res.*, 2005, **38**, 504.
146 G. Hummer and A. Szabo, *Proc. Natl. Acad. Sci. U. S. A.*, 2001, **98**, 3658.
147 A. N. C. Harris, Y. Song and C. H. Kiang, *Phys. Rev. Lett.*, 2007, **99**, 068101.
148 J. Preiner, H. Janovjack, C. Ranki, H. Knaus and D. A. Cisneros, *Biophys. J.*, 2007, **93**, 930.
149 W. Liu, V. Montana, V. Parpura and U. Mohideen, *Biophys. J.*, 2008, **95**, 419.
150 T. Ando, N. Kodera, E. Takai, D. Maruyama, K. Saito and A. Toda, *Proc. Natl. Acad. Sci. U. S. A.*, 2001, **98**, 12468.